Stress Intensity Factor Analysis of Interface Crack using Boundary Element Method*
(Application of Virtual Crack Extension Method)

Noriyuki MIYAZAKI**, Toru IKEDA**,
Toshihiro SODA** and Tsuyoshi MUNAKATA**

This paper presents a new method for stress intensity factor analysis of a two-dimensional interface crack between dissimilar materials. In the present paper, the virtual crack extension method which is a powerful tool for evaluating the stress intensity factor is combined with the boundary element method. A stress analysis is carried out using the boundary element method, and then virtual finite elements are assumed around a crack tip. The nodal displacements of these virtual finite elements are evaluated as internal points of a boundary element analysis. At first, we applied the present method to a center-cracked homogeneous plate under tension. Furthermore, we analyzed a bimaterial plate with a center interface crack and a bimaterial plate with a center slant interface crack subjected to tension. In such mixed mode problems, the M_1-integral was applied to the mode-separation to obtain the individual mode stress intensity factors. It is found from these analyses that the present method gives very accurate results whose accuracy is insensitive to the size of virtual finite elements.

Key Words: Boundary Element Method, Finite Element Method, Stress Intensity Factor, Fracture Mechanics, Virtual Crack Extension Method, Interface Crack, Mixed Mode

1. Introduction

Interface structures can be seen in various engineering fields such as those dealing with composite materials, adhesive joints and electrical components. From a viewpoint of the structural integrity of such interface structures, the assessment of interface fracture is very important, because the origin of fracture in such structures is usually on the interface between dissimilar materials.

Williams[1] pointed out the oscillation of the stress in the immediate vicinity of an interface crack tip, and Rice and Sih[2] proposed the stress distributions near an interface crack tip. The estimation methods for actual interface structures using the finite element method have been investigated by many authors. Yau and Wang[3] analyzed mixed mode stress intensity factors using the M_1-integral which was extended from the J-integral. Also, Matos et al.[4] obtained the stress intensity factors using the virtual crack extension method in conjunction with the principle of the M_1-integral, and Sun and Jih[5] proposed the application of the crack closure integral method to an interface crack. In the former two methods, the stress intensity factors of the individual fracture modes can be obtained, but in the latter one, mode-separation is impossible.

On the other hand, Yuuki and Cho[6] proposed an extrapolation method using the displacement field near a crack tip obtained from a boundary element analysis to determine the stress intensity factors of a bimaterial interface crack. Their method provides mixed mode stress intensity factors.

In previous papers[7],[8], the present authors applied the virtual crack extension method to stress intensity factor analysis using the combination of the boundary element method and the finite element method. In this method, finite elements were allocated only around the vicinity of a crack tip, and boundary elements were used to discretize the rest of a structure.

In this paper, extending the above method, we propose a new method for calculating the stress inten-

* Received 1st July 1992, Paper No. 91-0083 A
** Department of Chemical Engineering, Faculty of Engineering, Kyushu University, 6-10-1 Hakozaki, Higashi-ku, Fukuoka 812, Japan

sity factors, in which virtual finite elements whose nodal points consist of the internal points and the boundary nodes of a boundary element analysis, are allocated around a crack tip instead of actual finite elements and the virtual crack extension method is applied to calculating the stress intensity factors. We will also show the effectiveness of the present method combined with the M_1-integral for the mixed mode stress intensity factor analysis of a bimaterial interface crack.

2. Stress Intensity Factors of a Bimaterial Interface Crack

For the coordinate system shown in Fig. 1, the stress distributions around the interface crack tip along $x_2=0$ are given by Rice and Sih[2] as follows.

$$\sigma_{22}(r,0)=\frac{1}{\sqrt{2\pi r}}\left\{K_I(a)\cos\left[a\ln\left(\frac{r}{l}\right)\right]-K_{II}(a)\sin\left[a\ln\left(\frac{r}{l}\right)\right]\right\} \quad (1)$$

$$\sigma_{12}(r,0)=\frac{1}{\sqrt{2\pi r}}\left\{K_I(a)\sin\left[a\ln\left(\frac{r}{l}\right)\right]+K_{II}(a)\cos\left[a\ln\left(\frac{r}{l}\right)\right]\right\} \quad (2)$$

where a is a bimaterial constant defined as

$$a=\frac{1}{2\pi}\ln\left[\left(\frac{\chi_1}{\mu_1}+\frac{1}{\mu_2}\right)\Big/\left(\frac{\chi_2}{\mu_2}+\frac{1}{\mu_1}\right)\right]$$

$$\chi_j=\begin{cases}3-4\nu_j & \text{(Plane strain)}\\ (3-\nu_j)/(1+\nu_j) & \text{(Plane stress)},\ (j=1,2)\end{cases} \quad (3)$$

where μ and ν are the shear modulus and Poisson's ratio, the subscripts 1 and 2 denote the quantities relevant to the materials 1 and 2, and l denotes an arbitrary length to normalize the distance r. K_I and K_{II} in Eqs. (1) and (2) are regarded as the stress intensity factors for modes I and II of a bimaterial interface crack. The quantity l should be taken as a fixed value even for different crack lengths in estimating the fracture toughness of a bimaterial interface crack, but in this paper we take l as the crack length $2a$ because of the convenience of normalizing the stress intensity factors. The reason for taking l as a fixed value in estimating an actual interface crack is discussed in another paper[9].

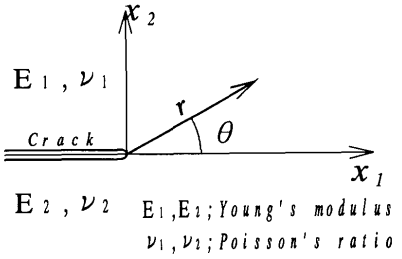

Fig. 1 The polar coordinates of a interface crack between dissimilar materials

The stress intensity factors are correlated with the energy release rate G by the following equations[10].

$$G=\beta(K_I^2+K_{II}^2)$$

$$\beta=\frac{1}{16\cosh^2(a\pi)}\left[\frac{\chi_1+1}{\mu_1}+\frac{\chi_2+1}{\mu_2}\right] \quad (4)$$

3. Numerical Analysis of a Bimaterial Interface Crack

3.1 The virtual crack extension method

The energy release rate G is obtained by the virtual crack extension method as follows[11].

$$G=-\left(\frac{\partial U}{\partial a}\right)\approx-\frac{1}{2}\sum_{i=1}^{N_F}\boldsymbol{u}_i^T\frac{\Delta \boldsymbol{k}_i}{\Delta a}\boldsymbol{u}_i \quad (5)$$

where U is the potential energy of the body, N_F is the number of finite elements, in which stiffness changes due to the virtual crack extension, $\boldsymbol{u}_i$ and $\boldsymbol{k}_i$ denote the nodal displacement vector and stiffness matrix of the element i, respectively, and the superscript T denotes the transpose of a vector. The differentiation of $\boldsymbol{k}_i$ with respect to crack length a is carried out by a small virtual crack extension.

3.2 Virtual finite element

In the usual application of the virtual crack extension method, displacement data are obtained from a finite element analysis and the energy release rate is calculated by a post processor of the virtual crack extension method as illustrated in the left side of Fig. 2.

In the method proposed here, we assume the virtual finite elements around the crack tip as shown in Fig. 3, whose nodes consist of the internal points and the boundary nodes of a boundary element analysis. The displacements of the internal points and the boundary nodes are obtained from the boundary element method. Then, the energy release rate is calculated using the same post processor for the finite element method as illustrated in the right side of

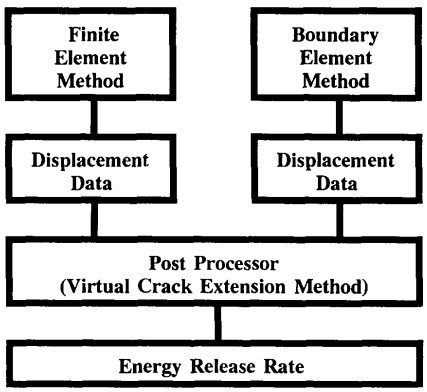

Fig. 2 The process of the virtual crack extension method in the cases of BEM and FEM

Fig. 2.

3.3 An analysis of a bimaterial interface crack using the virtual crack extension method

Unlike crack problems in homogeneous bodies, a bimaterial interface crack always induces both opening and sheering behavior even for single-mode loading. Thus it is necessary to evaluate each fracture mode of the stress intensity factor in order to characterize the behavior of a bimaterial interface crack. In this paper, the individual modes of stress intensity factors are obtained using the improved virtual crack extension method which was proposed by Matos et al.[4]. This method is based on the principle of M_1-integral proposed by Yau and Wang[3]. The concept of this method is briefly explained in the following section.

Consider two independent equilibrium states with field variables denoted by the superscripts (1) and (2) for the virtual finite elements region in an elastic body with an interface crack. The superscript (1) indicates the problem to be analyzed and the superscript (2) indicates the equilibrium state whose field variables and stress intensity factors are already known. The superposition of the two equilibrium states leads to another equilibrium state (1+2). The fields of stress and displacement of the superposed state can be written as

$$\begin{aligned} \boldsymbol{u}^{(1+2)} &= \boldsymbol{u}^{(1)} + \boldsymbol{u}^{(2)} \\ \boldsymbol{\sigma}^{(1+2)} &= \boldsymbol{\sigma}^{(1)} + \boldsymbol{\sigma}^{(2)} \end{aligned} \quad (6)$$

where $\boldsymbol{u}$ and $\boldsymbol{\sigma}$ denote the displacement vector and the stress tensor respectively. The stress intensity factors can also be superposed.

$$\begin{aligned} K_I^{(1+2)} &= K_I^{(1)} + K_I^{(2)} \\ K_{II}^{(1+2)} &= K_{II}^{(1)} + K_{II}^{(2)} \end{aligned} \quad (7)$$

By correlation of Eq.(7) with Eq.(4), the energy release rates of the state (1+2) are obtained as follows.

$$\begin{aligned} G^{(1+2)} &= \beta[(K_I^{(1+2)})^2 + (K_{II}^{(1+2)})^2] \\ &= G^{(1)} + G^{(2)} + 2\beta[K_I^{(1)}K_I^{(2)} + K_{II}^{(1)}K_{II}^{(2)}] \end{aligned} \quad (8)$$

Therefore,

$$2\beta[K_I^{(1)}K_I^{(2)} + K_{II}^{(1)}K_{II}^{(2)}] = G^{(1+2)} - G^{(1)} - G^{(2)} \quad (9)$$

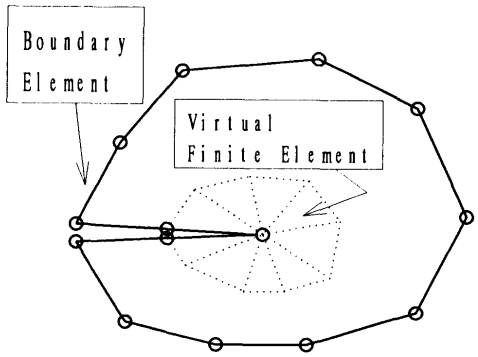

Fig. 3 Virtual finite elements around a crack tip

In Eq.(9), β, $K_I^{(2)}$, $K_{II}^{(2)}$ and $G^{(2)}$ are already known, and $G^{(1)}$ and $G^{(1+2)}$ are obtained from Eq.(5) using $\boldsymbol{u}^{(1)}$ and $\boldsymbol{u}^{(1+2)}$ as follows.

$$G^{(j)} = -\frac{1}{2}\sum_{i=1}^{N_F}(\boldsymbol{u}_i^{(j)})^T \frac{\Delta \boldsymbol{k}_i}{\Delta a}\boldsymbol{u}_i^{(j)} \qquad (j=1, 1+2) \quad (10)$$

The asymptotic solutions of the stress and displacement around an interface crack tip, which are shown in the Appendix, were used as the field variables of the known equilibrium state (2) in the present analysis. Considering $K_I^{(2)}=1$ and $K_{II}^{(2)}=0$, we obtain $K_I^{(1)}$ from Eq.(9) as

$$K_I^{(1)} = (G^{(1+2)} - G^{(1)} - G^{(2)})/2\beta \quad (11)$$

where the energy release rates $G^{(1+2)}$ and $G^{(2)}$ are evaluated using $K_I^{(2)}=1$ and $K_{II}^{(2)}=0$. If $K_I^{(2)}=0$ and $K_{II}^{(2)}=1$, the following equation can also be obtained from Eq.(9).

$$K_{II}^{(1)} = (G^{(1+2)} - G^{(1)} - G^{(2)})/2\beta \quad (12)$$

where $G^{(1+2)}$ and $G^{(2)}$ are evaluated using $K_I^{(2)}=0$ and $K_{II}^{(2)}=1$. Therefore, we can obtain the individual modes of stress intensity factors.

4. Numerical Results

4.1 A crack in a homogeneous material

The center cracked rectangular plate under uniform tension shown in Fig. 4 was analyzed for examining the reliability of the proposed method, in which the virtual crack extension method was applied to the virtual finite elements allocated around a crack tip, using the displacements obtained from a boundary element analysis. The stress intensity factor analyzed for the case of $a/W=0.5$ is normalized as $F_I = K_I/(\sigma_0\sqrt{\pi a})$, which is compared with Isida's solution[12].

Two types of crack extension schemes were examined. In the first type, the crack was extended by distorting the elements around the crack tip as shown in Type 1 of Fig. 5. In another type, the crack was extended by rigidly moving the core of elements around the crack tip and distorting the elements around this core as illustrated in Type 2 of Fig. 5.

In order to study the effects of the element size

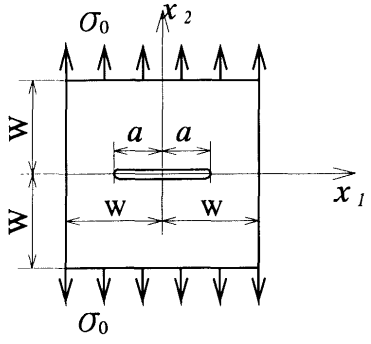

Fig. 4 A center cracked rectangular plate under uniform tension

near the crack tip on the accuracy of the stress intensity factor, analyses were carried out for various sizes of the virtual finite element around the crack tip, that is, m/a=0.5, 0.2, 0.1 and 0.05. Two examples of boundary element meshes for the cases of m/a=0.5 and 0.2 are shown in Fig. 6. The usual quadratic boundary elements with three nodes and two types of crack tip boundary elements were used in these analyses. One type of crack tip element, Type A, is made by shifting its mid-node to the quarter-point of the element as shown in Fig. 7, and the other one, Type B, is also made by shifting the mid-node as in Type A and by multiplying the shape function of traction by the following function expressing the traction singularity of $1/\sqrt{r}$[13].

$$x(r)=\frac{1}{\sqrt{r}}\left[1-\frac{r}{l_e}(1-\sqrt{l_e})\right] \tag{13}$$

where l_e is the length of the crack tip element and r is the distance from the crack tip. Both the elements can express the variation of the displacement around the crack tip which is proportional to $\sqrt{r}$, but only the Type B crack tip element can represent the singularity of the traction. Results of analysis under the conditions mentioned above are shown in Table 1. It can be seen from this table that the Type 1 crack extension scheme affects the accuracy of the results, while the Type 2 scheme provides very accurate results. In the case of the Type 2 scheme, the results of this analysis are not sensitive to the size of the boundary elements and the virtual finite elements around the crack tip. For example, the errors were very small even when extremely coarse mesh m/a=0.5 was used. An accurate stress intensity factor can be obtained using either Type A or Type B crack tip elements. The Type A crack tip element is recommended because of its simplicity. The results are omitted here, but in other cases of crack length, a/W=0.1~0.4, 0.6 and 0.7, the results obtained using the Type 2 crack extension scheme and Type A crack tip element agreed very well with Isida's. For all cases presented here, we chose Δa as $10^{-8}l$ or so, because the accuracy of the result is almost insensitive to the crack extension value.

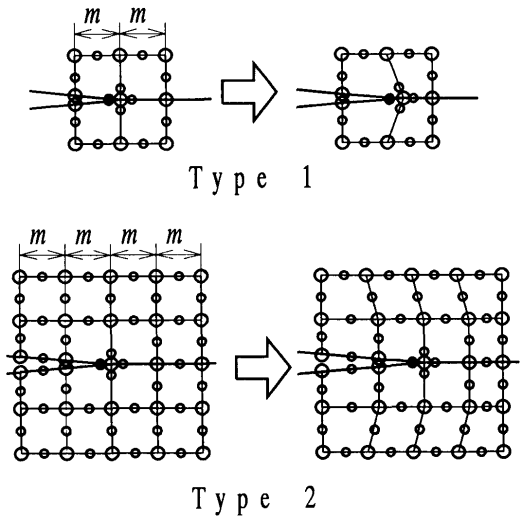

Fig. 5 Crack extension schemes

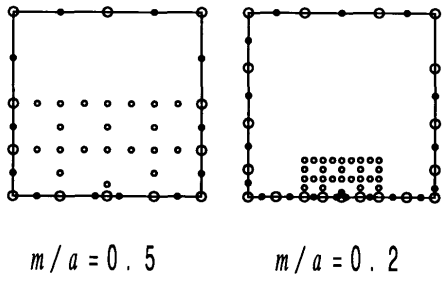

Fig. 6 Examples of the boundary element mesh

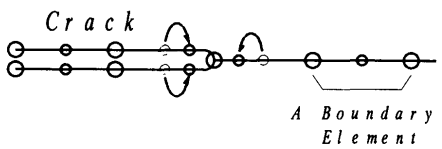

Fig. 7 Crack tip element

4.2 The stress intensity factors of a bimaterial interface crack

Several bimaterial interface crack problems were analyzed here. According to the guideline for homogeneous crack problems, we chose the Type 2 crack extension scheme and Type A crack tip element. Unlike a crack in a homogeneous material, the direction of the shear stress around a crack tip has a

Table 1 Normarized stress intensity factor of a center cracked rectangular plate under uniform tension (a/W=0.5)

Type of crack extension scheme	m/a			
	0.5	0.2	0.1	0.05
Type A crack tip element				
Type 1	1.365 (+2.3%)	1.355 (+1.6%)	1.351 (+1.3%)	1.349 (+1.1%)
Type 2	1.331 (−0.2%)	1.334 (0.0%)	1.333 (−0.1%)	1.333 (−0.1%)
Type B crack tip element				
Type 1	1.368 (+2.5%)	1.361 (+2.0%)	1.357 (+1.7%)	1.354 (+1.5%)
Type 2	1.330 (−0.3%)	1.333 (−0.1%)	1.333 (−0.1%)	1.333 (−0.1%)

( ): Relative error between present solution and Isida's.
Isida's solution: F_I=1.334 for a/W=0.5.

Table 2 Normalized stress intensity factors of a bimaterial plate with a center interface crack under uniform tension

Γ			a/W								
			0.1	0.2	0.3	0.4	0.5	0.6	0.7	0.8	0.9
1.0	Present solution	F_I	1.006	1.025	1.059	1.111	1.188	1.305	1.490	1.818	2.582
	Isida's solution	F_I	1.006	1.025	1.058	1.109	1.187	1.303	1.488	1.816	2.578
2.0	Present solution	F_I	1.001	1.020	1.053	1.104	1.181	1.296	1.478	1.799	2.546
		F_{II}	-0.072	-0.071	-0.071	-0.073	-0.077	-0.085	-0.100	-0.131	-0.214
	Yuuki's solution	F_I	0.996	1.019	1.053	1.104	1.180	1.294	1.477	1.798	2.546
		F_{II}	-0.072	-0.071	-0.072	-0.073	-0.078	-0.085	-0.100	-0.131	-0.214
3.0	Present solution	F_I	0.993	1.012	1.045	1.096	1.171	1.284	1.461	1.774	2.496
		F_{II}	-0.107	-0.106	-0.106	-0.109	-0.115	-0.127	-0.148	-0.193	-0.315
	Yuuki's solution	F_I	0.989	1.011	1.045	1.096	1.170	1.283	1.459	1.773	2.499
		F_{II}	-0.108	-0.106	-0.107	-0.110	-0.116	-0.127	-0.149	-0.193	-0.315
4.0	Present solution	F_I	0.987	1.006	1.039	1.089	1.163	1.273	1.446	1.752	2.460
		F_{II}	-0.129	-0.127	-0.127	-0.130	-0.137	-0.150	-0.176	-0.227	-0.368
	Yuuki's solution	F_I	0.983	1.005	1.038	1.088	1.162	1.272	1.445	1.751	2.460
		F_{II}	-0.129	-0.127	-0.127	-0.131	-0.137	-0.151	-0.176	-0.229	-0.369
10.0	Present solution	F_I	0.968	0.986	1.018	1.066	1.136	1.239	1.402	1.686	2.341
		F_{II}	-0.174	-0.171	-0.170	-0.173	-0.182	-0.198	-0.229	-0.293	-0.467
	Yuuki's solution	F_I	0.963	0.985	1.018	1.065	1.134	1.238	1.400	1.684	2.339
		F_{II}	-0.173	-0.170	-0.171	-0.174	-0.183	-0.199	-0.230	-0.295	-0.472
100.0	Present solution	F_I	0.946	0.964	0.994	1.039	1.104	1.201	1.351	1.612	2.213
		F_{II}	-0.206	-0.201	-0.200	-0.203	-0.210	-0.228	-0.260	-0.327	-0.514
	Yuuki's solution	F_I	0.940	0.962	0.994	1.038	1.104	1.201	1.349	1.610	2.209
		F_{II}	-0.205	-0.201	-0.201	-0.203	-0.211	-0.228	-0.260	-0.328	-0.519

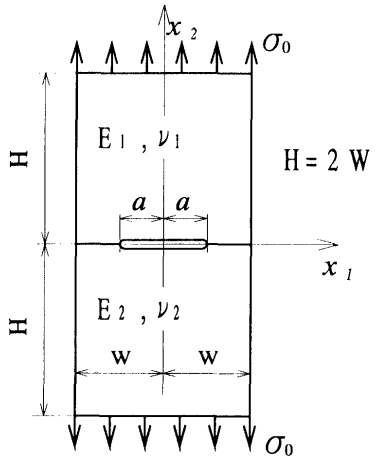

Fig. 8 A bi-material plate with a center interface crack under uniform tension

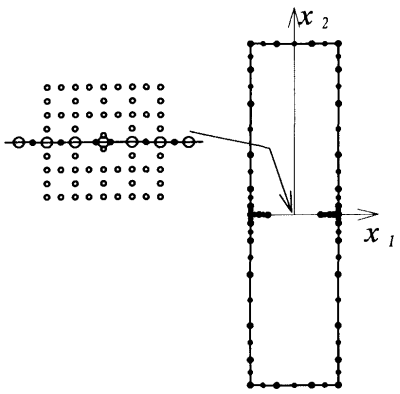

Fig. 9 A boundary element mesh of a bi-material plate with a center interface crack ($a/W=0.5$)

significant meaning for the fracture of a bimaterial plate with an interface crack. Thus we define the sign of the mode II stress intensity factor K_{II} as follows. The sign of K_{II} is determined for the coordinate system shown in Fig.1 where $E_1 \geq E_2$, and the sign of K_{II} is changed when $E_1 < E_2$.

4. 2. 1 A bimaterial plate with a center interface crack The first example is a bimaterial plate with a center interface crack under uniform tension as illustrated in Fig. 8. Considering the symmetry of the problem, the right half of the plate was modelled by the boundary elements. Analyses were carried out for the various ratios of Young's moduli $\Gamma(=E_1/E_2)$ and the various values of crack length a/W under the plane stress condition and $\nu_1=\nu_2=0.3$. An example of the boundary element model is shown in Fig. 9. The stress intensity factors obtained from the analyses are normalized as $F_I=K_I/(\sigma_0\sqrt{\pi a})$, $F_{II}=K_{II}/(\sigma_0\sqrt{\pi a})$.

The results obtained from the present analyses are compared with Isida's solutions[12] only for the

case of $\Gamma=1.0$ and Yuuki and Cho's solutions[6] for other cases, as shown in Table 2. The present solutions agree well with Isida's and Yuuki and Cho's. It is confirmed from these results that the virtual crack extension method combined with the boundary element method proposed in this study is very effective for a stress intensity factor analysis of a bimaterial interface crack problem.

4.2.2 A bimaterial plate with a center slant interface crack The second example is a bimaterial plate with a center slant interface crack under uniform tension as shown in Fig. 10. The stress intensity factors were obtained for the various ratios of Young's moduli $\Gamma=(E_1/E_2)$ and several crack angles θ under the plane stress condition, $\nu_1=\nu_2=0.3$ and $a/W=0.5$. Figure 11 is an example of the boundary element mesh. All of the results are shown in Figs. 12 and 13, in which the stress intensity factors are normalized the same way as in the case of a bimaterial plate with a center interface crack. It can be seen that the normalized mode I stress intensity factor F_I of the right side crack tip increases gradually but that of the left side crack tip decreases with the increase of Γ.

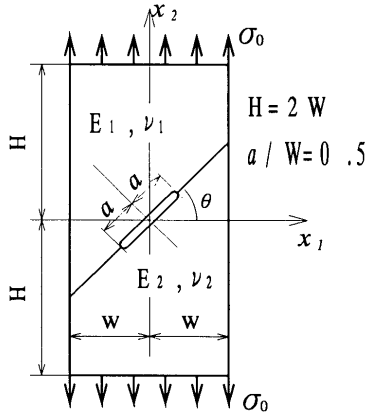

Fig. 10 A bi-material plate with a center slant interface crack under uniform tension

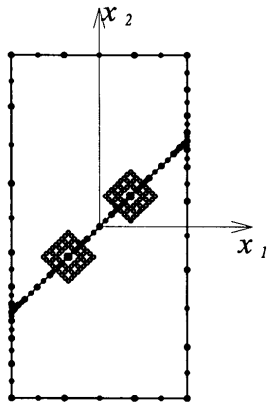

Fig. 11 Boundary element mesh of a bi-material plate with a center interface crack ($\theta=45°$)

The normalized mode II stress intensity factor F_{II} for the right side of the crack tip has a sign opposite to that for the left side of the crack tip. The absolute value of F_{II} of the right side crack tip decreases and that of the left side increases with the increase of Γ. In contrast to a crack in a homogeneous material, both crack tips have different stress intensity factors for interface cracks between dissimilar materials. It is interesting how this fact has an effect on the fracture behavior of a bimaterial interface crack.

5. Conclusions

(1) From several examples, it is confirmed that the virtual crack extension method combined with the boundary element method using the concept of the virtual finite element can be effectively applied to stress intensity factor analyses.

(2) The accurate stress intensity factors are obtained using the present method even when a coarse mesh around a crack tip is used.

(3) The present method combined with the M_1-integral provides accurate mixed-mode stress intensity factors for an interface crack between dissimilar materials.

(4) The post processor of the virtual crack

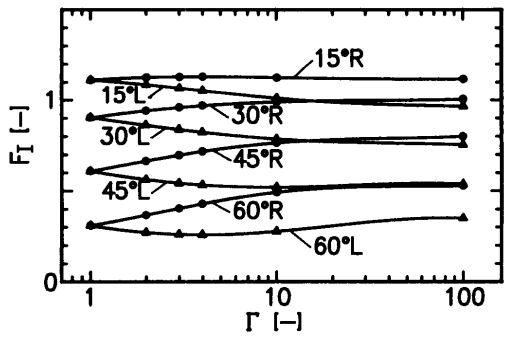

Fig. 12 Mode I stress intensity factor of a bi-material plate with a center slant interface crack (R: Right side tip of the crack, L: Left side tip of the crack)

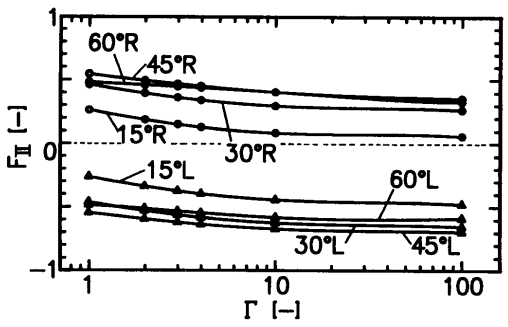

Fig. 13 Mode II stress intensity factor of a bi-material plate with a center slant interface crack (R: Right side tip of the crack, L: Left side tip of the crack)

extension method proposed in the present study is applicable to both the boundary element method and the finite element method.

Appendix

The following are the asymptotic solutions of stresses σ_{ij} and displacements u_i[5] for an interface crack between dissimilar materials, which hold in the vicinity of a crack tip in the polar coordinate system shown in Fig.7.

$$(\sigma_{11})_j = M_1\{K_I[f_{11}^I\omega_j - (1/\omega_j)\cos(\theta-\Theta)] + K_{II}[f_{11}^{II}\omega_j - (1/\omega_j)\sin(\theta-\Theta)]\} \quad (14)$$

$$(\sigma_{22})_j = M_1\{K_I[f_{22}^I\omega_j + (1/\omega_j)\cos(\theta-\Theta)] + K_{II}[f_{22}^{II}\omega_j + (1/\omega_j)\sin(\theta-\Theta)]\} \quad (15)$$

$$(\sigma_{12})_j = M_1\{K_I[f_{12}^I\omega_j - (1/\omega_j)\sin(\theta-\Theta)] + K_{II}[f_{12}^{II}\omega_j + (1/\omega_j)\cos(\theta-\Theta)\} \quad (16)$$

$$(u_1)_j = M_2\{K_I[x_j\omega_j h_{11} - (1/\omega_j)h_{12} + \omega_j h_{13}] + K_{II}[x_j\omega_j h_{21} - (1/\omega_j)h_{22} + \omega_j h_{23}]\} \quad (17)$$

$$(u_2)_j = M_2\{K_I[x_j\omega_j h_{21} - (1/\omega_j)h_{22} - \omega_j h_{23}] + K_{II}[-x_j\omega_j h_{11} + (1/\omega_j)h_{12} + \omega_j h_{13}] \quad (18)$$

$$M_1 = \frac{1}{2\sqrt{2\pi r}\cosh(\alpha\pi)}$$

$$M_2 = \frac{\sqrt{2\pi r}}{4\pi\mu_j\cosh(\alpha\pi)}$$

$$\alpha = \frac{1}{2\pi}\ln\left[\left(\frac{x_1}{\mu_1}+\frac{1}{\mu_2}\right)\Big/\left(\frac{x_2}{\mu_2}+\frac{1}{\mu_1}\right)\right]$$

$$\Theta = \alpha\ln\left(\frac{r}{l}\right)+\frac{\theta}{2}$$

$$x_j = \begin{cases} 3-4\nu_j & \text{(Plane strain)} \\ (3-\nu_j)/(1+\nu_j) & \text{(Plane stress)}, (j=1,2) \end{cases}$$

μ_j = Shear modulus

ν_j = Poisson's ratio

$\omega_1 = e^{-\alpha(\pi-\theta)}$, $\omega_2 = e^{\alpha(\pi+\theta)}$

$f_{11}^I = 3\cos\Theta + 2\alpha\sin\theta\cos(\theta+\Theta) - \sin\theta\sin(\theta+\Theta)$

$f_{11}^{II} = -3\sin\Theta - 2\alpha\sin\theta\sin(\theta+\Theta) - \sin\theta\cos(\theta+\Theta)$

$f_{22}^I = \cos\Theta - 2\alpha\sin\theta\cos(\theta+\Theta) + \sin\theta\sin(\theta+\Theta)$

$f_{22}^{II} = -\sin\Theta + 2\alpha\sin\theta\sin(\theta+\Theta) + \sin\theta\cos(\theta+\Theta)$

$f_{12}^I = 2\alpha\sin\theta\sin(\theta+\Theta) + \cos\theta\sin(\theta+\Theta)$

$f_{12}^{II} = 2\alpha\sin\theta\cos(\theta+\Theta) + \cos\theta\cos(\theta+\Theta)$

$h_{11} = [\cos(\theta-\Theta) - 2\alpha\sin(\theta-\Theta)]/(1+4\alpha^2)$

$h_{12} = [\cos\Theta + 2\alpha\sin\Theta]/(1+4\alpha^2)$

$h_{13} = \sin\theta\sin\Theta$

$h_{21} = [\sin(\theta-\Theta) + 2\alpha\cos(\theta-\Theta)]/(1+4\alpha^2)$

$h_{22} = [-\sin\Theta + 2\alpha\cos\Theta]/(1+4\alpha^2)$

$h_{23} = \sin\theta\cos\Theta$

where the subscripts $j(j=1,2)$ indicate respective materials comprising the bimaterial plate.

References

(1) Williams, M. L., The stress around a fault or crack in dissimilar media, Bull. Seismol. Soc. Am., Vol. 49, (1959), p. 199.

(2) Rice, J. R. and Sih, G. C., Plane problems of cracks in dissimilar media, Trans. ASME, J. Appl. Mech., Vol. 32, (1965), p. 418.

(3) Yau, J. F. and Wang, S. S., An analysis of interface cracks between dissimilar isotropic materials using conservation integrals in elasticity, Eng. Fract. Mech., Vol. 20, No. 3, (1984), p. 423.

(4) Matos, P. P. L., Mcmeeking, R. M., Charalambides, P. G. and Drory, M. D., A method for calculating stress intensities in bimaterial fracture, Int. J. Fract., Vol. 40, (1989), p. 235.

(5) Sun, C. T. and Jih, C. J., On strain energy release rates for interfacial cracks in bi-material media, Eng. Fract. Mech., Vol. 28, No. 1, (1987), p. 13.

(6) Yuuki, R. and Cho, S., Efficient boundary element analysis of stress intensity factors for interface cracks in dissimilar materials, Eng. Fract. Mech., Vol. 34, No. 1, (1989), p. 179.

(7) Miyazaki, N., Ikeda, T. and Munakata, T., Stress intensity factor analysis by combination of boundary element and finite element methods., Eng. Fract. Mech., Vol. 36, No.1, (1990), p. 61.

(8) Miyazaki, N., Ikeda, T. and Munakata, T., Stress intensity factor analysis by combination of boundary element and finite element methods (Application to axisymmetric crack problems), Proceedings of the twelfth International conference on boundary elements in engineering, Vol. 1, (1990), p. 255, Computational Mechanics Publications.

(9) Ikeda, T., Miyazaki, N., Soda, T. and Munakata, T., Mixed mode fracture criteria of interface crack between dissimilar materials, to be published in Trans. Jpn. Soc. Mech. Eng. (in Japanese), No. 92-0527.

(10) Malyshev, B. M. and Salganik, R. L., The strength of adhesive joints using the theory of cracks, Int. J. Fract., Vol. 1, (1965), p. 114.

(11) Parks, D. M., A stiffness derivative finite element technique for determination of crack tip stress intensity factors, Int. J. Fract., Vol. 10, (1974), p. 485.

(12) Isida, M., Effect of width and length on stress intensity factors of internally cracked plates under various boundary conditions, Int. J. Fract. Mech., Vol. 7, No. 3 (1971), p. 301.

(13) Cruse, T. A., Two-dimensional BIE fracture mechanics analysis, Appl. Math. Modelling, Vol. 2, (1978), p. 287.